Polymer Melt Rheology by Magnetic Resonance Imaging

Yusuf Uludag,[†] Michael J. McCarthy,[‡] Geoffrey A. Barrall,[§] and Robert L. Powell*[,†]

Department of Chemical Engineering & Materials Science, Department of Food Science & Technology, University of California, One Shields Avenue, Davis, California 95616, and Quantum Magnetics, Inc., 7740 Kenamar Court, San Diego, California 92121-2425

Received September 6, 2000

ABSTRACT: A magnetic resonance imaging (MRI) tubular rheometer for polymer melt systems is described. This technique allows the viscosity to be determined over a range of shear rates. It relies upon obtaining steady-state velocity profiles in tubular pipes using MRI and simultaneously measuring the pressure drop. In these experiments, the shear viscosity of a low-density polyethylene (LDPE) melt was measured at shear rates between 1.8 and 12.1 s^{-1} and was found to be approximately 117.7 Pa•s. The viscosity was also determined using a parallel plate rheometer in which it was found to vary slightly with shear rate, ranging from 113.9 to 107.2 Pa•s, comparing favorably with the MRI determined values. MRI is noninvasive and nondestructive and can be applied to opaque systems; hence, it has the potential to be used for in-process monitoring.

Introduction

The rheological behavior of polymer melts plays a strong role in their processing and is often indicative of other properties such as molecular weight or, in the case of filled systems, microstructure. The most commonly characterized property is the shear viscosity which generally varies with shear rate and hence needs to be determined over a wide range of shear rates. The principal techniques for characterizing polymer melt viscosity are off-line and require that samples be drawn from a particular point or at various stages of a process and subsequently analyzed in a laboratory. Such methods produce viscosity data over a range of shear rates; however, these procedures are labor-intensive and require a long time to complete. Rapid in-line or on-line analysis is needed to improve real time control of polymer processing.

On-line and in-line viscosity measurement methods are commercially available. They potentially offer process monitoring, quality control, and automatic process control[1] which are important in improving both process economics and end product quality. For on-line measurements a side stream is analyzed, whereas in-line devices are installed at a particular point in the process itself. Most of the available on-line or in-line rheometers measure steady shear viscosity at a single shear rate.[2] A few rheometers utilize a pump to drive the process stream through a number of parallel capillaries, providing measurements at more than one shear rate. Increasing the number of data points requires changing the flow rate by adjusting the pump speed. An alternative, and we believe better, approach would characterize the melt over a wide range of shear rates while avoiding the need for multiple capillaries or auxiliary pumping or if, for example, multiple capillaries are used, more comprehensively exploit their characteristics. Specifically, in capillary flow, the polymer melt experiences shear rates that theoretically range from zero at the center of the capillary to a maximum at the wall. If it were possible to provide a local measurement of viscosity, then, from a single capillary experiment, it would be possible to determine the viscosity over a range of shear rates—a methodology that we call pointwise observations for rheological characterization.[3,4]

Measuring the viscosity by this method involves using velocity profiles determined in fully developed steady tube flow and an auxiliary measurement of the pressure drop. The latter is related to shear stress distribution, $\sigma(r)$, through conservation of linear momentum,

$$\sigma(r) = -\frac{\Delta P}{2L} r \tag{1}$$

where $\Delta P/L$ is the pressure gradient. The velocity profile $v(r)$ provides the means of determining shear rate distribution, $\dot{\gamma}(r)$,

$$\dot{\gamma}(r) = \left|\frac{dv(r)}{dr}\right| \tag{2}$$

By eliminating r in eqs 1 and 2, one can determine the shear stress vs the shear rate, or the shear viscosity, η, at points inside the tube from the usual definition of the viscosity.

$$\sigma(\dot{\gamma}) = \eta(\dot{\gamma})\,\dot{\gamma} \tag{3}$$

In recent years, we developed the idea of pointwise rheological observations using magnetic resonance imaging as our probe for tube flow.[3−5] Quantitative flow measurements can be obtained from MRI using either time-of-flight[6−8] or phase encode imaging.[9−14] Time-of-flight velocity imaging involves building a velocity image by successively exciting a particular cross section of the flow and detecting the arrival of the excited spins at a downstream cross section. By precisely knowing the downstream location of the detected signal and the time between excitation and detection, a velocity profile can be constructed for laminar, unidirectional flow. Phase encoding produces direct images of velocity distributions for both unidirectional and more complex flows. Magnetic field gradients are applied to encode the position

[†] Department of Chemical Engineering & Materials Science, University of California.
[‡] Department of Food Science & Technology, University of California.
[§] Quantum Magnetics, Inc.

10.1021/ma001543w CCC: $20.00
Published on Web 06/27/2001

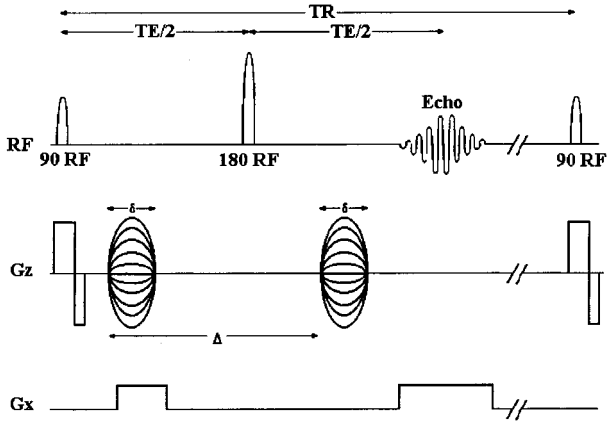

Figure 1. Pulsed-gradient spin-echo pulse sequence for flow imaging.

and the displacement rate of the spins in terms of frequency and phase of the signal originating from the spins, respectively. A two-dimensional Fourier transform of the signal produces a map that is the conditional probability density of a fluid element at a certain position and displacement velocity.

In our previous studies,[3−5] this technique was used to determine the shear viscosity of polymer solutions over nearly three decades of shear rates from a single measurement. Here, we present the first attempt to determine the shear viscosity of a polymer melt using MRI. The results agree with those obtained from an independent measurement of viscosity. It is important to recognize that this technique does not rest on a correlation or on an independent calibration.

Experimental Section

The MRI system consists of a General Electric CSI-II (General Electric Medical Systems, Fremont, CA)/TecMag Libra spectrometer (TecMag, Houston, TX) connected to a 0.6 T Oxford superconducting magnet with a 0.33 m bore diameter. The magnetic field gradient coils are driven by an Oxford-2339 water-cooled gradient power amplifier. A standard pulsed-gradient spin-echo pulse sequence, shown in Figure 1, was used to generate a data set of size 256 × 64 in which the transverse or *x* position was frequency encoded while the axial velocity was phase encoded. Echo time (TE) and repetition time (TR) were 50 ms and 2 s, respectively. In a typical experiment the spatial and velocity resolutions were 0.25 and 0.9 mm/s, respectively.

The flow system consisted of a steel tube of length 1.07 m and a quartz tube of length 0.915 m. The inside diameters of the tubes were 12.7 mm. Flanges and high-temperature O-rings were employed to provide a smooth joint between the steel and quartz tube. A pilot scale single-screw extruder, Killion KL-075 (Cedar Grove, NJ), was connected to the steel tube to pump the polymer melt through the system. The temperature of the system was monitored and regulated via temperature controllers, Omega CN4400 (Stamford, CT), that were connected to resistive heating wires placed around the steel tube and covered by glass wool for insulation. Heating of the quartz tube section of the flow system, shown in Figure 2, was achieved by blowing hot air through the annular space between the quartz tube and a glass tube of larger diameter. Pressure measurements were made using a digital pressure display (Dynisco 1400, Franklin, MA) connected to a pressure sensor that was mounted at the connection between the steel and the quartz tube. Pressure-hole errors, considered small for concentrated polymer solutions and polymer melts,[15] were neglected in all calculations.

Low-density polyethylene (Sclair, Canada) with a melting temperature of 108 °C and melt index of 51.5 was used for these experiments in which a polymer melt temperature of 232 °C (±2 °C) was maintained. The molecular weights M_w, M_n, and M_z are 52 000, 24 000, and 137 000, respectively. The viscosity of the polymer melt was measured at 232 °C using 25 mm parallel plate viscometer (Rheometrics Ares rheometer, Piscataway, NJ). These results are presented in Figure 3.

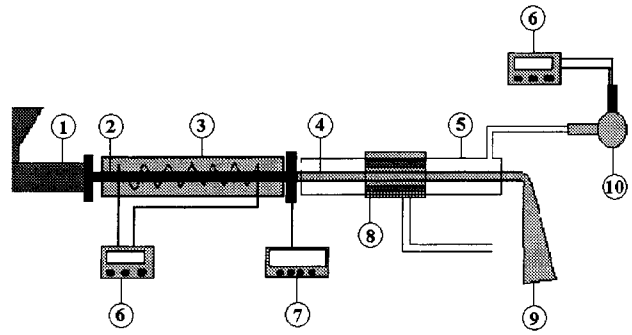

Figure 2. Polymer melt flow system: 1, extruder; 2, steel tube; 3, glass wool insulation; 4, quartz tube; 5, glass tube insulation; 6, temperature controller; 7, pressure display; 8, rf coil; 9, polymer melt; 10, heat gun.

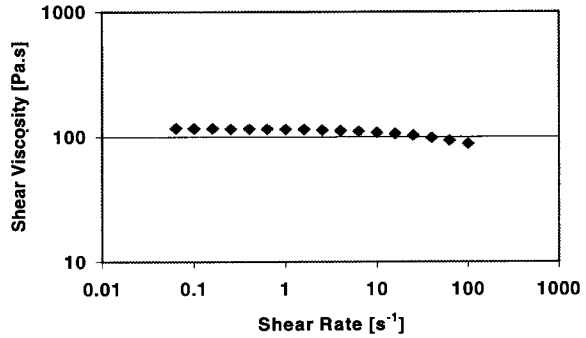

Figure 3. Shear viscosity of the polymer melt obtained by using a parallel plate rheometer.

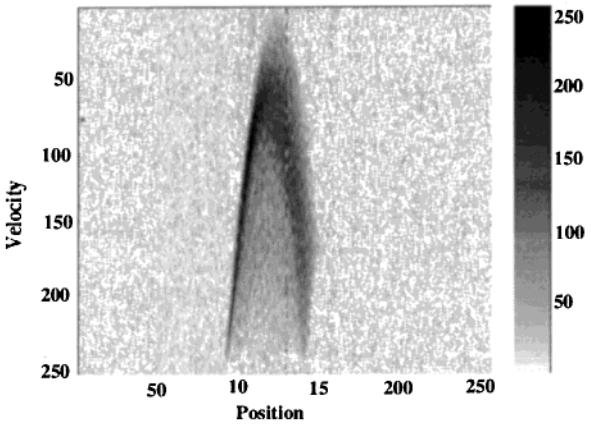

Figure 4. Velocity profile of the LDPE melt in tube flow obtained using MRI. The intensity is scaled between 1 and 256.

Results and Discussion

Figure 4 shows a typical phase encode image obtained after zero filling the data set to 256 × 256. Increasing the number of data points in the phase encoding direction from 64 to 256 by zero filling results in a dimension of 0.23 mm/s per pixel. In Figure 4, the velocity is represented along the vertical axis and the radial position along the horizontal axis. The figure is the probability distribution of finding spins at a particular location and velocity. Dark regions imply that

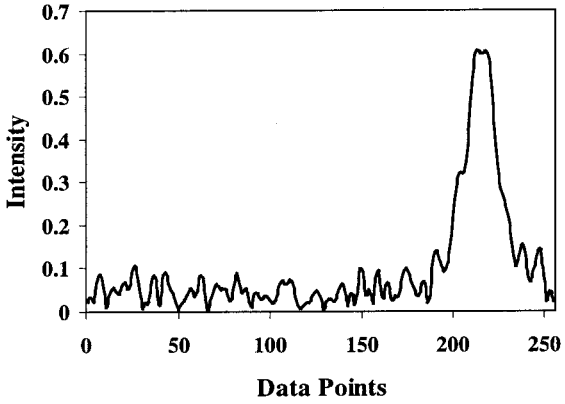

Figure 5. Signal intensity distribution at the radial position of 5.5 mm.

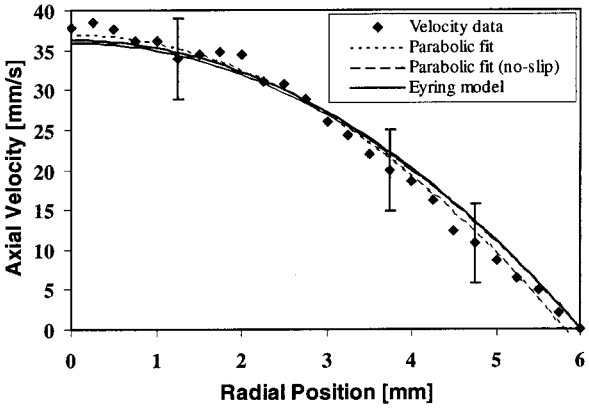

Figure 6. Velocity profile data fitted by parabolic functions and the Eyring model. The error bars represent one standard deviation of the MRI signal intensity.

the probability is high. Light regions indicate a low probability for a particular velocity at a given position x. A 2D FT of the data acquired in the experiment described yields the projection of this distribution along the x axis. For laminar pipe flow, one can take the ridge of the 2D probability distribution as the velocity profile, $v(r)$. If the ridge is not sharp, this can lead to problems. The nonzero signal amplitude interior to the ridge is due to the projection operation. The signal-to-noise ratio was negatively affected by the 44 ms spin−spin relaxation time of the polymer melt, which is shorter than the echo times of approximately 50 ms. Another feature of the image is that it has been reconstructed to remove aliasing effects. Aliasing in the flow occurs when the maximum velocity exceeds half of the velocity field of the view either in the positive or negative direction. Aliasing does not pose any problem in reconstructing the velocity profile. In fact, aliasing improves the velocity resolution without increasing the imaging time.[16]

With all of these limitations, it is still possible to obtain the velocity profile by identifying the maximum signal intensity at each radial position of the velocity image. An example of this is shown in Figure 5, which gives the signal intensity at the radial position vs velocity represented by pixel 95. Most of the signal intensity is at pixel 213, corresponding to a velocity of 4.8 mm/s. Similar analyses are performed at each radial position until the velocity as a function of radius is constructed.

Once the velocity profile is found, the next step is to calculate the shear rate. In our earlier studies[3−5] a general even-order polynomial fit was used to smooth the velocity profiles. The resulting equation was then differentiated to obtain the shear rate. The objective of these earlier studies was to determine whether a wide range of non-Newtonian behavior could be measured by the pointwise method. The fluids that were used in those studies showed shear thinning or yield stresslike behavior, and in some cases, a range of shear rates was observed over which the fluids exhibited a constant viscosity. By assuming a general polynomial form for the velocity, we were able to capture this behavior without biasing the data toward a particular constitutive model. In the present experiments, the system was operated at low flow rates to prevent polymer melt leakage at the joint between the steel and the quartz tube. An average velocity of 19 mm/s was used, giving rise to shear rates ≤ 12 s^{-1}. Figure 3 shows that the LDPE is nearly Newtonian with only slight shear thinning being found at shear rates greater than 1 s^{-1}. For example, for shear rates between 1 and 10 s^{-1}, the viscosity decreases by less than 5%. Such small changes in the viscosity give rise to subtle deviations from the Newtonian velocity profile. Further, the data in the present experiments are not as accurate as those obtained in the previous experiments due to the circumstances mentioned in the Experimental Section. As such, we selected a priori to attempt to fit the velocity profile to a parabolic form and compare the resulting viscosity with the data in Figure 3. We chose two methods to fit the data. First, we simply assumed

$$v = a + b\left(\frac{r}{R}\right)^2 \tag{4}$$

and allowed the constants a and b to vary. This does not account for the no-slip condition. All points are given equal weight, and the fit near the wall does not represent the physical situation. The result of this analysis is shown in Figure 6 with $a = 37$ mm/s and $b = -40$ mm/s. The second part of this analysis using parabolic velocity profile specified the no-slip condition with the result shown in Figure 6, with the maximum velocity being 36 mm/s.

As indicated by eq 2, we now differentiate the velocity profile and combine this information with the shear stress distribution to obtain the local shear viscosity. To determine the shear stress distribution, the pressure drop is measured and combined with eq 1. Under ideal circumstances, two pressure transducers are placed along the tube over a region where the flow is fully developed. The total measured normal stress gradient is equal to the isotropic pressure gradient. In this study pressure measurement was made only at a single point in the flow system. The pressure drop was found by assuming that the fully developed flow regime persists to the very end of the tube and that end effect can be represented through an exit pressure. That is, rather than assuming that the exit pressure was atmospheric, we corrected for elastic effects using literature values of the exit pressure for a LDPE melt,[15] 172.2 kPa. The resulting shear stress distribution found through eq 1 is $\sigma(r) = 0.24r$, where σ is in kPa and r is in mm, with the pressure drop being 476.3 kPa/m.

Assuming that the velocity profile is parabolic implies an assumption of constant viscosity. Both the shear stress and the shear rate are linear in radius, and dividing the two empirical expressions yields a constant

Table 1. Viscosity Values Obtained by MRI Using Parabolic Fit with Both Slip and No-Slip Boundary Conditions for Both Corrected and Uncorrected Exit Pressure

method	viscosity [Pa·s]
corrected	108.3
corrected and no-slip	117.7
uncorrected	125.1
uncorrected and no-slip	136.2

viscosity. The values that were obtained by this procedure are given in Table 1. Also shown in this table are values for the viscosity that would be obtained if there were no correction for the exit pressure error. To compare these results with the data shown in Figure 3, we must identify the range of shear rates over which these data are expected to be valid. Ideally, the shear rate varies from zero at the tube center to a maximum value at the wall. Because of the finite spatial and velocity resolutions for MRI, there is a limit to the observable minimum shear rate. In a previous study,[17] a correlation was established between the minimum detectable shear rate and the experimental conditions. Using this correlation, the minimum shear rate that can be detected under the parameters of this study is estimated to be 1.8 s^{-1}. The maximum shear rate is 12.1 s^{-1}, representing a range of shear rates covering nearly 1 decade. Over this range, Figure 3 shows that the viscosity varies from 113.9 to 107.2 Pa·s. Comparing these values with those of Table 1, an error of approximately 7% is seen. Further, the total amount of shear thinning is about 6%, implying that the assumption of Newtonian behavior is reasonable over this range of shear rates.

Another approach to this analysis is to assume a form of the velocity profile that is not parabolic and undertake a full pointwise analysis, as was done previously.[3−5] As discussed above, this approach is confounded by the slight amount of shear thinning observed in the data shown in Figure 3 as well as the poorer resolution of the MRI data than those from our previous studies. As such, we apply an alternative analysis to attempt to capture some of the shear thinning character but without the generality of the previous studies. Using a straight polynomial fit cannot capture the functional behavior of the LDPE data. A polynomial fit of the velocity profile implies that that a polynomial fit of the viscosity data themselves is reasonable. This may work fine for shear thinning materials with a lower Newtonian plateau. However, when the amount of shear thinning is small, such fits are not robust in that they do not represent the shear thinning as monotonic or may predict a stronger dependence of the viscosity upon shear rate than that actually observed. Models such as the power law, Bird−Carreau,[18] and Ellis[19] are inadequate because they do not permit the shear thinning to be slight over a wide range of shear rates. One model that allows behavior such as that shown in Figure 3 is the Eyring model[19]

$$\eta = \frac{\tau_0}{\dot{\gamma}} \sinh^{-1}(\tau_0 \dot{\gamma}) \tag{5}$$

where τ_0 is a characteristic time. The corresponding velocity field is

$$v = \frac{R}{\tau_0 \sigma_w} \cosh \sigma_w - \frac{R}{\tau_0 \sigma_w} \cosh \frac{\sigma_w r}{R} \tag{6}$$

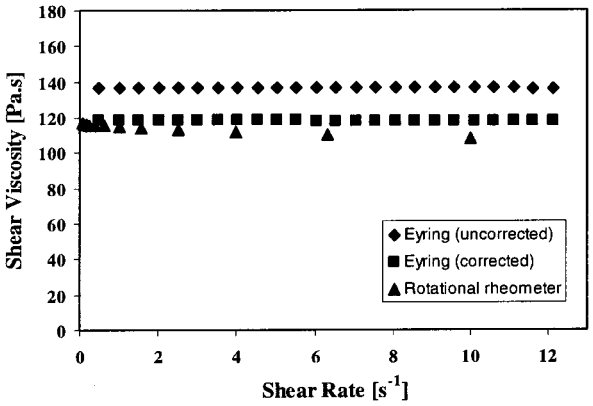

Figure 7. Polymer melt viscosity vs shear rate by the Eyring model with and without the exit pressure correction.

where σ_w is the wall shear stress. Figure 6 shows the fit to the velocity data using eq 6, and Figure 7 shows the corresponding shear viscosities using no end correction and with the end correction. Almost 15% difference between the results clearly indicates that using an exit pressure value to be used in pressure drop calculation has an important effect on the viscosity results. It also shows that we are able to capture some slight shear thinning behavior. As seen in Figure 6, the three fitted velocity profiles are nearly indistinguishable; within the errors of this experiment, they all give the same results.

The viscosity results obtained by using different fits to smooth the velocity data compare well with each other and with the conventional rheometer results when exit pressure correction is applied. The viscosities calculated by assuming that the exit pressure is atmospheric are significantly higher. In practical applications, measuring the pressure at two different points will directly provide the pressure drop. With an experimental setup to obtain higher quality images and higher shear rates, it will be possible to use polynomial fits without resorting to different constitutive models to express the velocity data. In our earlier studies,[3−5] we have shown that this approach yielded highly accurate viscosity measurements.

Conclusions

Magnetic resonance imaging was used to determine the velocity profile of a LDPE melt in tube flow. This profile was analyzed to calculate the local shear rate and, when combined with a pressure drop measurement, the local viscosity. For the data in this study, the amount of shear thinning was sufficiently small as to permit the fluids to be treated as Newtonian over the shear rate range accessed by the flow system. The viscosity obtained was within 7% of that found using a parallel plate viscometer. The sole limitation throughout the experiments was that the flow system could not withstand higher pressures associated with higher flow rates than that reported. Modifying the flow system to be able to operate at higher flow rates, and hence at high shear rates, and to attach one more pressure transducer for direct measurement of the pressure drop should lead to an on-line viscosity sensor for polymer melts and other non-Newtonian fluids that permits the shear viscosity to be determined over a wide shear rate range in a single measurement taking approximately 2 min, as we have shown for a variety of polymer solutions.[3−5]

Acknowledgment. This work was supported by grants from the Department of Energy (DE-FG07-96ER14727) and the National Science Foundation (NSF-9661122) and the Center for Process Analytical Chemistry, University of Washington. The authors acknowledge the support of the DuPont Corporation, the gracious willingness of Dr. Glenn Heffner and Patricia M. Cotts in providing the data in Figure 3 and molecular weight values, and the valuable assistance of Dr. Serge Bobroff during the experiments.

References and Notes

(1) Dealy, J. M.; Wissbrun, K. F. *Melt Rheology and Its Role in Plastics Processing: Theory and Applications*; Van Nostrand Reinhold: New York, 1990.
(2) Dealy, J. M. *Chem. Eng.* **1984**, *91*, 62−70.
(3) Powell, R. L.; Maneval, J. E.; Seymour, J. D.; McCarthy, K. L.; McCarthy, M. J. *J. Rheol.* **1994**, *38*, 1465−1470.
(4) Arola, D. F.; Barrall, G. A.; Powell, R. L.; McCarthy, K. L.; McCarthy, M. J. *Chem. Eng. Sci.* **1997**, *52*, 2049−2057.
(5) Arola, D. F.; Powell, R. L.; Barrall, G. A.; McCarthy, M. J. *J. Rheol.* **1999**, *43*, 9−30.
(6) McCarthy, K. L.; Kauten, R. J.; McCarthy, M. J. *J. Food Eng.* **1992**, *16*, 109−125.
(7) Altobelli, S. A.; Givler, R. C.; Fukushima, E. *J. Rheol.* **1991**, *35*, 721−734.
(8) Sinton, S. W.; Chow, A. W. *J. Rheol.* **1991**, *35*, 735−772.
(9) Majors, P. D.; Givler, R. C.; Fukushima, E. *J. Magn. Reson.* **1989**, *85*, 235−243.
(10) Abbott, J. R.; Tetlow, N.; Graham, A. L.; Altobelli, S. A.; Fukushima, E.; Mondy, L. A.; Stephens, T. S. *J. Rheol.* **1991**, *35*, 773−795.
(11) Graham, A. L.; Altobelli, S. A.; Fukushima, E.; Mondy, L. A.; Stephens, T. S. *J. Rheol.* **1991**, *35*, 191−201.
(12) Seymour, J. D.; Maneval, J. E.; McCarthy, K. L.; McCarthy, M. J.; Powell, R. L. *Phys. Fluids A* **1993**, *5*, 3010−3012.
(13) Gibbs, S. J.; James, K. L.; Hall, L. D. *J. Rheol.* **1996**, *40*, 425−440.
(14) Britton, M. M.; Callaghan, P. T. *Magn. Reson. Chem.* **1997**, *35*, 37−46.
(15) Han, C. D. *Rheology in Polymer Processing*; Academic Press: New York, 1976.
(16) Arola, D. F.; Barrall, G. A.; Powell, R. L.; McCarthy, M. J. *J. Magn. Reson. A* **1997**, *3*, 175−184.
(17) Arola, D. F.; Powell, R. L.; Barrall, G. A.; McCarthy, M. J. *Rev. Sci. Instrum.* **1998**, *69*, 3300−3307.
(18) Bird, R. B.; Carreau, P. J. *Chem. Eng. Sci.* **1968**, *23*, 427−434.
(19) Bird, R. B.; Armstrong, R. C.; Hassager, O. *Dynamics of Polymeric Liquids*; John Wiley & Sons: New York, 1987.

MA001543W